Low-frequency variability in the Southeastern Pacific

A. Vega [1], Y. Du Penhoat [1], B. Dewitte [1],
O. Pizarro [2], R. Abarca [3]
[1] (LEGOS, France)
[2] (PROFC, Chile)
[3] (CS, France)

We study the propagation and forcing of baroclinic Rossby waves in the eastern South Pacific Ocean from TOPEX/POSEIDON and ERS-1/2 altimetric data (TP/ERS). A quasi-geostrophic lineal model is used to evaluate both wind and coastal forcing in that region. Preliminary results show long Rossby waves propagating from the South American coast to the interior of the ocean. At annual periods, these waves are generated at the coastal boundary by the annual fluctuation of the alongshore wind stress. At interannual periods most of the variability along the coast is of equatorial origin. These coastal oscillation generate interannual Rossby waves that propagate the coastal signal, and hence ENSO variability, to the interior of the South Pacific Ocean.

The eastern boundary of the South Pacific Ocean is a region of strong coastal upwelling with one of the highest levels of biological productivity of the world. The regular coastal upwelling is associated with the Southeastern Pacific Subtropical Anticyclone, which produces northerly winds at the coast (figure 1). Deep and rich-nutrient waters fertilize coastal upper waters, making the fisheries off Peru and Chile the most productive of the Eastern boundary currents with annual landings accounting for approximately 15% of the world marine catch [FAO, 1993]. Local and equatorial-forced coastal trapped waves (CTWs), which propagate poleward along the South American coast, are responsible for a large part of the variability of coastal currents, sea level and density field at intra and interannual time scales [Shaffer et al. 1997, 1999]. Remote-forced CTWs are related to equatorial Kelvin waves, which are most prominent during the Southern Hemisphere Summer and during the onset of ENSO events [Kessler et al., 1995]. The zonal transference of coastal variability to the open ocean is principally related to the westward propagation of extra-equatorial Rossby waves (RWs). The surface signature of baroclinic RWs can be observed from satellite altimetry, from which their propagating characteristics can be investigated.

Our objective is to study the propagation and forcing of baroclinic long RWs in the southeastern Pacific from TOPEX/POSEIDON and ERS-1/2 (TP/ERS) data. A quasi-geostrophic lineal model is used to interpret the observations. Preliminary results indicate that equatorial perturbations at ENSO timescales propagate efficiently to the interior of the South Pacific through RWs forced by low-frequency fluctuation along the coast.
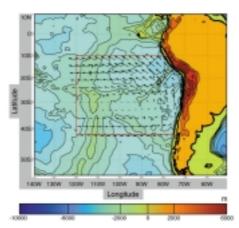

Figure 1: The southeastern Pacific topography and mean wind stress from ERS-1/2 for the 1992-2000 period (black arrows). The red box represents the zone under investigation. Wind data were provided by CERSAT (Brest).
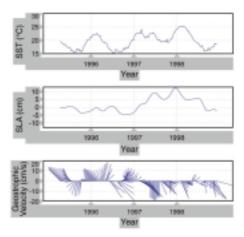

Figure 2: Time series of sea surface temperature, sea level anomalies and geostrophic currents estimated from TP/ERS near the coast at 15°S (TP/ERS data processed as in [Ducet et al., 2000])

Results

Figure 2 shows the time series for sea surface temperature (SST), sea level height anomalies (SLA) and TP/ERS-derived geostrophic velocity anomalies near the coast (200 km offshore) at 15°S. Positive sea level anomalies were observed at the beginning of 1997. They were associated with southward geostrophic flow anomalies. These fluctuations were related to the strong 1997-98 El Niño, which led to positive SST anomalies of about 5°C near the coastal region.

An Extended EOF (E-EOF) analysis of altimetric data yields three distinct modes of variability (figure 3). The first and most energetic mode contains about 28% of the total variance and is associated with the low-frequency 1997-98 El Niño variability. The spatial structure shows larger amplitudes at lower latitudes and near the coast. The second mode accounts for about 20% of the total variance and is a combination of an interannual and an annual mode. The third mode comes out as a pair (the other

element of the pair is not shown), indicating that it is a propagating mode at the annual period. The pair accounts for 21% of the variance with a structure of large amplitude extending from the central eastern Pacific at low latitude to near the coast at higher latitudes. The zone of positive values becomes narrower with increasing latitude, suggesting they are associated with RW propagation from the coast (the higher the latitude, the slower the phase speed and the smaller the Rossby radius of deformation).

With propagation speeds of about 250 km/day [Shaffer et al., 1997], the fast CTWs—produced by equatorial Kelvin waves impinging the South American coast—generate a large fraction of low-frequency coastal sea level variability, leading to an elevation or depression of the pycnocline. For instance, during the 1982-83 El Niño and the 1997-98 El Niño, the 13°C isotherm near the northern Chilean coast was depressed by more than 200 metres [Blanco et al., 2001]. Through RWs, this low-frequency disturbance propagated westward from the coast with phase speeds in agreement with linear RW theory (not shown). Figure 4 shows the TOPEX/ POSEIDON sea level anomalies between Caldera (27°04'S; 70°50'W) and Eastern Island (27°09'S; 109°27'W) for the 1992-1998 period. Large sea level anomalies in 1997-1998 associated with the interannual Kelvin waves in the tropical Pacific [Delcroix et al., 2000] propagate from the coast. The RWs decreased in amplitude as they propagated westward because of local wind forcing, advection, diffusion and other processes. A linear model forced by the ERS winds and sea level at the coast was used to assess the role of local wind forcing in changing the RW propagating characteristics. Figure 5 shows the longitude-time plots of wind curl
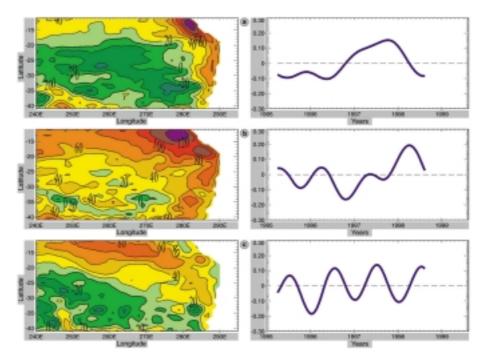

Figure 3: Three first leading E-EOFs (Extended EOFs) of sea level anomalies from TP/ERS. Left panels show the spatial structures of the modes and the right panels the associated time series. We use a time window of one year with a one-month interval (time resolution is 10 days). This lead to a $3x12xN_x xN_y$-dimensional "observation" vector, where N_x and N_y are the numbers of longitude and latitude grid points respectively ($N_x=56$, $N_y=31$). The variance maximization procedure for these extended vectors leads to the diagonalization and eigenvalue problem of the lagged-covariance matrix. Percentages of explained variance are indicated at the top of each panel. Multiplying the time series with the amplitude of the spatial structure yields the value in millimetres for sea level for the corresponding mode. Contour interval is 10 units.
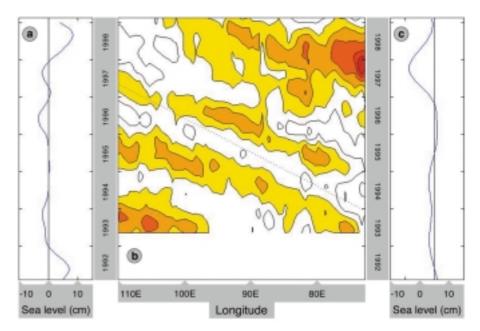a) 1st EOF (28.29%); b) 2nd EOF (20.11%) and c) 3rd and 4th EOF (21.40%)

Figure 4: Sea level at a) Caldera (27°04'S 70°50'W and c) eastern island (27°09'S, 109°27'W. b) Low-passed, interannual TOPEX/POSEIDON sea level anomalies near 27°S from the South American coast to 110°W for the period indicated in the figure. Dashed line indicates the slope of the curve related to a perturbation propagating with the phase speed of a long Rossby wave ($\beta c^2/f^2$, where β and c are the meridional gradient of f, the Coriolis parameter and the first-mode long wave speed—about 2.3 m/s in the region—respectively).

stress, pycnocline depth estimated from TP/ERS SLA, the output of the quasi-geostrophic linear model and sea level time series from the tide gauge at 18°S. The wind curl (figure 5a) exhibits a clear seasonal cycle, also present in the SLA. Note that the seasonal fluctuations in SLA (figure 5b) are also related to a steric effect due to seasonal changes in sea temperature. During the 1997-98 El Niño, a large depression of the pycnocline took place. The induced anomalies propagated westward with a phase speed value close to linear theory. Model results and observations are comparable from the coast up to 90°W at annual and ENSO timescales when friction is used in the model. The time decay for the friction is close to one year, which led to the best agreement between observations and the model. West of 90°W, the model simulation exhibits smaller variability than the observations because of local forcing and other processes not taken into account (i.e. non-linearities).

Conclusions

The annual and interannual southeast Pacific baroclinic RWs are generated at the coast by the fluctuations of pycnocline related to the passing of CTWs.
Their propagation characteristics are altered by the local wind stress curl and non-linearities. The impact

of the 1997-98 El Niño event was clear, with the presence of an energetic RW between 1997 and 1998. Since these RWs may efficiently propagate offshore, they may modify the strength of the circulation and the thermal structure near the surface and the water properties at large spatial scales in the Southern Pacific. Our aim is to determine the forcing of these waves in order to connect local and equatorial

fluctuations with extra-tropical variability. An important effort will also be devoted to the study of the interaction of the Antarctic Circumpolar Current (ACC) system, which may also influence the variability of this region. General circulation model simulations are now under investigation for the analysis of climate variability in Southern America induced by these teleconnections.
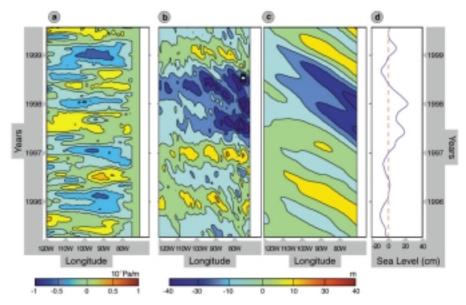

Figure 5: Longitude-time plot at 18°S of wind curl stress from ERS-1/2 (in 10^{-7} Pa/m) (provided by CERSAT) (a) pycnocline depth anomalies estimated from TP/ERS (m) (b) pycnocline depth anomalies from a quasi-geostrophic linear model (m) (c) and sea level anomalies at the coast from tide gauge data (cm) (provided by TOGA Sea Level Center) (d). Negative values for pycnocline depth anomalies correspond to a deepening of the thermocline and a warming of the surface waters. The model was forced by the ERS-1/2 winds and its boundary conditions in the east correspond to thermocline depth anomalies along the South American coast between 10°S and 40°S. They were given by a high-resolution Eastern Boundary linear Model (EBM) forced by sea level data at the equator [Pizarro et al., 1999].

References

Blanco J.L., A.C. Thomas, M.E. Carr, and P.T. Strub, 2001: Seasonal climatology of hydrographic conditions in the upwelling region off northern Chile, *J. Geophys. Res.* (submitted).

Delcroix T., B. Dewitte, Y. Du Penhoat, F. Masia and J. Picaut, 2000: Equatorial waves and warm pool displacement during the 1992-1998 El Niño events. *J. Geophys. Res.*, 105, 26,045-26,062.

Ducet N., P.Y. Le Traon and G. Reverdin, 2000: Global high-resolution mapping of ocean circulation from TOPEX/POSEIDON and ERS-1/2. *J. Geophys. Res.* (in press).

FAO, 1993: FAO Yearbook of fisheries statistics, 1991. Yearbook of Fishery Statistics, Vol. 73. Food and Agricultural Organization of the United Nations, Rome.

Kessler W. S., M.J. McPhaden and K. Weickmann, 1995: Forcing of intraseasonal Kelvin waves in the equatorial Pacific. *J. Geophys. Res.*, 100, 10 613-10 632.

Pizarro O., A.J. Clarke and S.V. Gorder, 1999: El Niño sea level and currents along the South American coast: comparison of observations with theory. *J. Phys. Oceanogr.* In press.

Shaffer G., O. Pizarro, L. Djurfeldt, S. Salinas and J. Rutllant, 1997: Circulation and low-frequency

variability near the Chile coast: Remotely-forced fluctuations during the 1991-1992 El Niño. *J. Phys. Oceanogr.*, 27, 217-235.

Shaffer G., S. Hormazabal, O. Pizarro, S. Salinas, 1999: Seasonal and interannual variability of currents and temperature off central Chile. *J. Geophys. Res.*, 104, C12, 29,951-29,961.

Corresponding author:
Andres Vega Martin
LEGOS
14, av. Edouard Belin
31400 Toulouse Cedex 4 - France
E-mail: andres.vega@cnes.fr